ROYAL SOCIETY OF CHEMISTRY

Check for updates

Influence of *Spinacia oleracea* leaf extract concentration on silver nanoparticle formation and evaluation of antimicrobial properties

Tamara Akpobolokemi,[a] Etelka Chung,[c] Rocio Teresa Martinez-Nunez,[b] Guogang Ren, [ID][c] Bahijja Tolulope Raimi Abraham [ID] *[a] and Alex Griffiths [ID][d]

Plant mediated nanofabrication is a sustainable strategy for generating biocompatible nanomaterials with diverse industrial applications. Despite growing interest, there remain notable gaps in the understanding of the influence of plant extract concentration on the physiochemical properties of silver nanoparticles (AgNPs), particularly regarding their size. Conflicting reports suggest an increase in AgNP size with increased extract concentration, and others suggest the opposite. To address this, this study explores the influence of varying *Spinacia oleracea* (*S. oleracea*) leaf extract concentrations on the physiochemical properties of AgNPs and their antimicrobial activity against Gram negative (*Escherichia coli*), Gram positive (*Staphylococcus aureus*, *Streptococcus pyogenes*) bacteria and Fungi (*Candida albicans*). Hence, our investigation encompasses persistent infection-causing microorganisms currently plagued with drug resistance issues. This study's findings will enhance understanding of this sustainable nanofabrication approach, highlighting AgNP's potential application as novel antimicrobial agents. Results confirmed spherical nanoranged AgNPs were synthesised, obtaining AgNP-2%, AgNP-3%, AgNP-4%, AgNP-7%, and AgNP-10% v/v *S. oleracea* leaf extract. Our analysis revealed a consistent trend of size reduction with increasing extract concentration: AgNP-2% (173 nm), AgNP-3% (211 nm), AgNP-4% (148 nm), AgNP-7% (120 nm), and AgNP-10% (109 nm). Regarding antimicrobial activity, the lower concentration AgNPs (AgNP-2% and AgNP-3%) showed no activity, while all the higher concentrations AgNPs displayed full inhibition of all tested microbes. In summary, our research emphasises the significance of plant extract concentration in optimising AgNP synthesis and size reduction. The demonstrated antimicrobial properties suggest promising applications in industries such as environmental (water purification), biomedical (wound healing, drug delivery), and agricultural (pesticides, water remediation).

Introduction

Metallic nanoparticles have gained increased traction over the years due to their excellent chemical, optical,[1] electrical, catalytic properties and applications in a variety of fields, including therapeutics.[2–4] However, while efficient, traditional chemical nanofabrication methods have raised several concerns, including toxicity, use of non-eco-friendly materials,

[a] King's College London, School of Cancer and Pharmaceutical Sciences, Institute of Pharmaceutical Science, Waterloo Campus, Franklin Wilkins Building, Stamford Street, London SE1 9NH, UK. E-mail: bahijja.raimi-abraham@kcl.ac.uk
[b] King's College London, Department of Infectious Diseases, School of Immunology & Microbial Sciences, Faculty of Life Sciences & Medicine, King's College London, Guy's Hospital, London, UK
[c] School of Physics, Engineering and Computer Science, University of Hertfordshire, Hatfield AL10 9AB, UK
[d] London Metallomics Facility, Faculty of Life Sciences & Medicine, King's College London, London SE1 9NH, UK. E-mail: alexander.1.griffiths@kcl.ac.uk

and high production costs.[5] As the demand for metallic nanoparticles and research grows in this area, more robust, sustainable, and cost-effective nanofabrication methods are required.[6–8] Green approaches for manufacturing metallic nanoparticles offer several advantages over chemical methods, including sustainability, cost-effectiveness, and biocompatibility.[9,10] Green synthesis is a promising alternative, utilising microorganisms (*e.g.* bacteria, fungi) or biochemicals present in plant or fruit extracts to synthesise stable metallic nanoparticles.[11–13] Unlike other biological methods, plant-mediated synthesis eliminates the need for microorganism culturing and maintaining favourable aseptic conditions, making it an attractive choice for large-scale production.[14,15] Plant mediated synthesis offers a cost effective, one-pot synthesis method that leverages phytochemicals naturally present in plants to both reduce and stabilise the metallic ion, yielding well-formed stable nanoparticles.[16,17] The major role of phytochemicals in plant mediated synthesis of metallic

nanoparticles has been established by multiple studies.[16,18–20] These phytochemicals include flavonoids, terpenoids, phenols, and tannins.[21] They have key functional groups, including hydroxyl, carboxylic, ethers and esters groups, that are involved in the bioreduction of the metal salts and their subsequent stabilisation.[18,20,21]

The way in which this may occur is illustrated in Fig. 1, using the phytochemical quercetin as an example. As shown in Fig. 1, the hydroxy groups present in quercetin lead to the reduction of Ag^+ to Ag^0. Following this, the reduced outcome Ag^0 is stabilised by carboxylic groups resulting from the oxidation of the hydroxyl groups in the reduction process. This leads to the effective formation of stable AgNPs.

Illustration adapted from ref. 22.

Despite plant mediated synthesis undeniable advantages, it has limitations, including challenges related to upscaling production and a restricted shelf life due to the involvement of biological components. However, these limitations can be effectively addressed through approaches such as additional functionalisation, the incorporation of stabilising agents to enhance shelf life, the selection of plant species readily available for large-scale production and the optimisation of experimental conditions.[23–25] The success of plant mediated synthesis is dependent on this optimisation, and various experimental parameters can influence this, including temperature, pH, incubation time, and extract concentration.[16,24,26,27] These factors play crucial roles in shaping the physicochemical properties of the resultant nanoparticles. For example, studies have found that reduced extract pH and an acidic reaction environment led to the formation of larger particles.[24,28] Whereas in higher alkaline pH levels, a reduction in particle diameter was observed.[24,28] It has been suggested that this extract pH dependent size influence occurs due to the preference of nanoparticles to aggregate in lower pH levels rather than nucleate as observed in higher pH levels[28] Regarding temperature, studies have reported higher temperatures facilitate faster creation of nanoparticles with smaller sizes and uniform population distribution.[29,30] All these establish that these parameters discussed are crucial in determining the properties of the nanoparticles generated. Of particular interest in this study is the extract concentrations, as it has been shown to significantly affect metallic nanoparticles' size, shape, and antimicrobial behaviour[31,32] Nonetheless, even with the established importance of extract concentration, there is a significant knowledge gap regarding its role in nanoparticle synthesis and its subsequent therapeutic potential.

Little is understood about how variations in extract concentration can impact nanoparticle size, composition, and antimicrobial activity. Specifically, there have been mixed reports regarding extract concentration influence on size. Given that nanoparticle size is a critical parameter affecting solubility, stability, and cell interactions, understanding the relationship between extract concentration and size is essential.[33,34] Smaller nanoparticles are known to have larger surface area, which increases water solubility and improves stability.[35,36] In drug delivery, variations in nanoparticle size have also been demonstrated to significantly affect nanodrug interactions with cells and the number of therapeutic molecules delivered per cell. Hence, developing nanoparticles of suitable sizes is paramount. In the literature, with the use of plant mediated nanoparticle synthesis, some studies have revealed a size increase of nanoparticles with increased extract concentration.[37,38] However, other studies have reported a contrary relationship where increased extract concentration led to
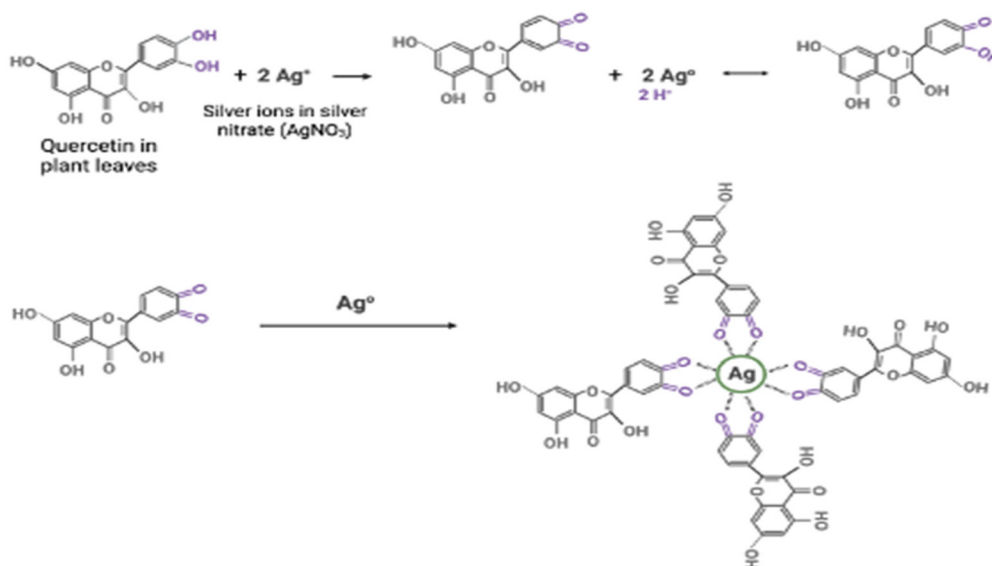
Fig. 1 The reduction and stabilisation of silver ions by quercetin using its hydroxyl and carboxylic groups, respectively. The silver ions in green (Ag^+) are firstly reduced by the hydroxylic group, leading to the formation of Ag^0. The reduction process forms carboxylic groups, which then effectively stabilises the reduced silver ion Ag^0. Groups that are major players in this process are highlighted in purple.

smaller particles being formed.[39,40] As such, these contradictory reports in the existing literature necessitate further investigations. Besides size, increased extract concentration has also been reported to facilitate increased plasmonic absorbance and generation of nanoparticles.[41] Lastly, studies investigating extract effects on antimicrobial activity have generally demonstrated higher concentrations of the extract leading to increased antibacterial effects.[42,43] These findings underscore the critical role that extract concentration plays not only in nanoparticle synthesis but also in the functional properties and therapeutic application of the resultant nanoparticles.

Resultant metallic nanoparticles synthesised using plant mediated synthesis offer room for medical applications as therapeutic agents.[44,45] Various metallic nanoparticles with therapeutic potential and antimicrobial activity have been generated using plant mediated synthesis. For example, gold nanoparticles generated using *Pyrenacantha grandiflora* extracts[46] were active against beta lactamase producing *Klebsiella pneumonia*.[46] Notably, *K. pneumonia* is a significant contributor to the burden of drug resistance and the proliferation of lung pneumonia.[47] AgNPs have also been generated using plant leaf extracts with exceptional antimicrobial activity.[31] In fact, studies comparing the antimicrobial activity of gold nanoparticles *versus* that of AgNPs demonstrated the possibility of increased antimicrobial effect with AgNPs.[48–50] Hence, the generation of plant derived AgNPs is the focus of this study. This choice of metal ion also stems from the fact that silver (Ag) has a long history in traditional medicine, as its characterised by high antimicrobial activity and reduced toxicity in animal cells.[51,52] Several examples exist of Ag-based products being used as an antimicrobial agent in various clinical applications, including coating of surgical tools[53] and wound healing.[54]

As aforementioned, plant mediated AgNPs have been shown to have a good spectrum of therapeutic and antimicrobial activity, which can be applied to various biomedical sciences. With their proven efficacy as anticancer,[11] antiviral,[55] and antibacterial agents.[56,57] In this regard, this study aims to investigate the influence of *S. oleracea* leaf extract concentrations on the size, composition, and antimicrobial activity of AgNPs. *S. oleracea* was chosen in this study because it contains rich flavonoids covering quercetin, myricetin, kaempferol, and apigenin, which contributes to its ability to facilitate plant mediated synthesis of metallic nanoparticles.[58,59] It is also commonly available, accessible, and cost effective. To the best of our knowledge, the concentration of ethanolic extracts of *S. oleracea* leaves and their influence on the physiochemical and antimicrobial properties of AgNPs have not been investigated. In this study, AgNPs were fabricated using various concentrations of the *S. oleracea* leaf extract and the influence of the extract concentration on the physiochemical (size, shape, composition) properties and antimicrobial activity of AgNPs against *C. albicans*, *S. aureus*, *E. coli*, and *S. pyogenes* was confirmed. These were chosen to assess the inhibitory effect of the AgNPs in a broad spectrum of microbial targets, namely: Gram negative (*E. coli*), Gram positive bacteria (*S. aureus*,

S. pyogenes), as well as fungi (*C. albicans*). They are also common infectious pathogens causing various infections that can be invasive and life threatening, including necrotising soft tissue infections, endocarditis, and pharyngitis.[60–62] Moreover, *S. aureus*, *E. coli*, *S. pyogenes* and *C. albicans* collectively contribute to a significant global healthcare challenge due to increasing drug resistance issues.[63–66] Hence, the generated AgNPs may offer alternative novel treatment options.

Materials and methods

Materials

Silver Nitrate ($AgNO_3$) (Catalogue number: 204390) and absolute Ethanol (≥99.8%) (Catalogue number: 34852-M) were purchased from Merck UK (Origin Country: Germany). Resazurin dye, the appropriate broths (namely nutrient broth for bacteria, yeast peptone dextrose broth for fungi) and antimicrobial agents (gentamicin and clotrimazole) were purchased from Merck UK (Origin Country: Germany). *S. oleracea* leaves (Fig. 2) (originally from Spain) were procured from a local grocery store in London, United Kingdom.

Method

Preparation of *S. oleracea* leaf extract. Before use, all laboratory apparatus were washed with tap water before use and then rinsed with distilled water. To enable consistency in the synthesis process, young *S. oleracea* leaves were used throughout this study. *S. oleracea* leaf extract was obtained using the infusion extraction process, which involves the extraction of compounds from plant material suspended in the chosen solvent and allowed to step over a defined time period.[67] The solvent used in our work was a 1 : 1 mix of ethanol and water. Bi-component extractions, including organic solvents such as ethanol, have been more effective than mono-component extractions.[68,69]

The method, in brief, used 10 g of freshly obtained washed *S. oleracea* leaves; these were washed with tap water and then distilled water. The leaves were cut into smaller sizes and immersed in equal parts ethanol (50 ml) and distilled water
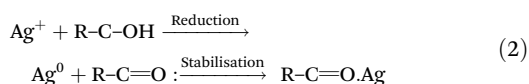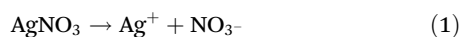

Fig. 2 *S. oleracea* (green spinach) leaves.

mix (50 ml) for 15 hours. The *S. oleracea* extract was obtained the following day by filtering out the leaves. Following this, the *S. oleracea* extract was purified firstly by centrifugation at 7000 RPM for 10 min and then, secondly, by filtration using a grade 1 Whatman filter.

Generation of AgNPs using *S. oleracea* leaf extract. A similar method used by Fatimah *et al.*, 2019 was slightly modified and applied to this study.[37] AgNPs were generated by mixing varied volumes of *S. oleracea* leaf extract with a 1 mM solution of $AgNO_3$. It is suggested that the plant mediated formation of AgNPs occurs through the following.[70] $AgNO_3$, the Ag ion donor, disassociates to provide Ag cation (Ag^+). The Ag^+ then reacts with plant phytochemicals, which reduces it to Ag^0. The reduced Ag ion is then stabilised by the same phytochemicals to form AgNPs. Eqn (1) and (2), shows the representative chemical equation for the synthesis process.

Eqn (1) and (2). Process of plant-mediated synthesis of AgNPs:

$$AgNO_3 \rightarrow Ag^+ + NO_3^- \tag{1}$$

$$Ag^+ + R\text{–}C\text{–}OH \xrightarrow{\text{Reduction}}$$
$$Ag^0 + R\text{–}C\text{=}O : \xrightarrow{\text{Stabilisation}} R\text{–}C\text{=}O.Ag \tag{2}$$

NB: R is representative of other components of the plant material.

Adapted from ref. 71.

In this study, AgNPs were generated by adding 2, 3, 4, 7 and 10% v/v *S. oleracea* leaf extract to a 1 mM solution of $AgNO_3$. Resultant nanoparticles are referred to as AgNP 2%, AgNP 3%, AgNP 4%, AgNP 7% and AgNP 10%. Control samples (AgNP-2 & AgNP-10%) were achieved by mixing equal parts ethanol: distilled water with $AgNO_3$ at the desired extract concentrations without *S. oleracea* leaf extract. To increase the rate of reduction of Ag^+ to Ag^0, following the addition of *S. oleracea* leaf extract to $AgNO_3$, the mixtures were placed on a magnetic stirrer at 300 rpm, and a temperature of 70 °C was set. The experiment ran for 3 hours to allow the effective formation of the AgNPs as longer reaction times have been associated with nanoparticles with favourable physiochemical properties.[72,73] Following the synthesis of AgNPs, to remove any unbound reactants and impurities, the nanoparticles were purified by centrifugation for 15 min at 15 000 rpm. Following this, the supernatant was discarded, and the nanoparticle pellet suspended in 1 ml ultra-pure water. This process was repeated twice, and the samples suspended in 1 ml water were stored in the fridge at 4 °C for further analysis.

Characterisation

UV-visible spectroscopy (UV–Vis). UV-visible is a characterisation technique that measures the plasmon absorbance of electrons on AgNPs using electromagnetic radiation in the visible light region.[74] The plasmon absorbance of AgNPs is responsible for the yellowish colour that develops following synthesis, providing a visual confirmation.[75] AgNPs are known to produce absorbance peaks around 390–450 nm when exposed to visible light.[76,77] As such, the presence of the peak around this area in the analysis is indicative of the presence of the synthesised AgNPs. The spectral absorbance of the samples was taken using a PerkinElmer Lambda 2 UV-Vis spectrophotometer, scanned from 300–600 nm, and the blank solution was distilled water. Spectra were plotted using GraphPad Prism 9.4.1.

Scanning electron microscopy (SEM). SEM provides a morphological assessment of the physical properties of synthesised nanoparticles. The signals derived from the scanning provide information on both the surface topography (size and shape) as well as the chemical composition (SEM-Energy Dispersive Xray) of the sample.[78] The morphology of AgNPs was studied using an FEI Quanta 200 FEG SEM for imaging at 5–10 kV accelerating voltage using secondary electron detection. A fragment of the sample was attached to a self-adhesive carbon disc mounted on a 25 mm aluminium stub. The stub was coated with 10 nm of gold using a sputter coater. The stub was then placed into the SEM. The film was allowed to dry on the SEM grid, and analysis was done afterwards. Image J version 1.53 s was used to calculate the size of the nanoparticles.

Dynamic light scattering (DLS). DLS studies were conducted as part of the morphological analysis (Z-average, polydispersity index (PDI)) of the synthesised AgNPs. A Malvern Nanosizer ZS was used for the study with refractive index and absorption values of 0.135 and 3.99, respectively. Analytical determinations were made in triplicate. All experimental data are expressed as mean ± standard deviation.

Attenuated total reflectance – Fourier-transform infrared spectroscopy (ATR-FTIR). ATR-FTIR is a technique that measures the absorbance of electromagnetic radiation of the samples in the mid-infrared region (4000–400 cm^{-1}).[79] Hence, the ATR-FTIR spectra analysis was used to determine the molecular composition and major functional groups in the plant mediated synthesis of the AgNPs. Perkin Elmer's ATR-FTIR spectrometer was used at a resolution of 4 cm^{-1}, with 32 scans conducted at 4000–600 cm^{-1}. The background scan was first conducted on the empty, cleaned (with ethanol), sample area before analysing the AgNP samples and *S. oleracea* leaf extract. The ATR-FRIR spectra were obtained thrice to ensure reproducibility. The spectra data were then analysed and plotted using graph pad prism 9.4.1.

Inductively coupled plasma mass quadrupole spectrometry (ICPQMS). The samples were diluted by a factor of 4000–40 000x by serial dilution using 0.7 M HNO_3 to a total volume of 15 mL. A calibration standard was made volumetrically using a 100 mg L^{-1} Sigma Aldrich TraceCert multi-element standard, and a 0.7 M HNO_3 stock solution was made from Optima grade concentrated HNO_3 (67–69% w/w; Fisher Scientific) and purified water with a resistivity ≥18.2 MΩ cm from a Milli-Q system (Merck Millipore). All the measurements were undertaken using a PerkinElmer NexION 350D ICP-QMS under Kinetic Energy Discriminator (KED) mode. The introduction system to the instrument was a Cetac ASX-520 auto-sampler coupled to a SeaSpray glass nebuliser fitted to a

quartz cyclonic spray chamber. Argon plasma flow and nebuliser gas flow rates were 18 L min^{-1} and 0.93 L min^{-1}, respectively.

Antimicrobial analysis. Evaluations were conducted using the resazurin broth method widely employed in antimicrobial studies.[80,81] This is based on the ability of viable respiratory cells to reduce blue coloured resazurin to pink resorufin.[82] Hence, the absence of a colour change is an indication of the bactericidal activity of the nanoparticles. The antimicrobial activity of the synthesised AgNPs was tested on *E. coli*, *S. aureus*, *S. pyogenes* and *C. albicans* (ATCC 2091). All microbes used were obtained from The University of Hertfordshire microorganism collection and grown in a shaking incubator (200 rpm at 37 °C) for 24 hours in broth (Nutrient broth for bacteria, yeast peptone dextrose broth for fungi), respectively. The microbes were diluted to ~3 × 10^7 colony forming units per ml (CFU ml^{-1}) in Mueller Hinton broth using CE 1021 spectrophotometer (Cecil) at 600 nm. The nanoparticles were vortexed for about 10 seconds, then kept in a sonic bath for 1 minute, vortexed again, and kept in the sonic bath for a further 1 minute. In a 96 well plate, 100 μL of microbes were treated with 100 μL of nanoparticles to make a final concentration of 1.25 × 10^9 particles per ml. The negative control was the broth, while the microbes without nanoparticle treatment were the positive control. In addition, antimicrobial controls were added: gentamicin (10 μg ml^{-1}) for bacteria and clotrimazole (10 μg ml^{-1}) for fungi. The plates were then incubated at 37 °C for 24 hours. Following incubation, 25 μL of resazurin dye (0.02%) was added to each well and incubated again for 24 hours. The colour change was observed and recorded.

Result

## Visual confirmation of synthesised AgNP

The reduction of Ag$^+$ to Ag^0 and synthesis of the AgNPs was confirmed by a colour change, from light green to yellowish-brown, as shown in Fig. 3, other studies have also reported this occurrence.[83,84] It can also be seen in Fig. 3, that there was no change in colour in both of the controls (2% and 10%), as they remained colourless throughout the reaction.

Nanoparticle composition analysis using UV-Vis

Following the visual representation of the synthesis of AgNPs, UV-Vis spectroscopy technique was employed to examine the absorption spectrum of samples within the UV-Vis light range. This method, as also indicated by Akash and Rehman in 2019,[74] is instrumental in validating the synthesis and existence of AgNPs by detecting their Surface Plasmon Resonance (SPR) effect. The SPR effect is a phenomenon resulting from the interaction of light with the free electrons present in metal nanoparticles, as elucidated by.[85,86] This occurrence induces a resonant oscillation or vibration of valence electrons on the nanoparticle surface when exposed to an electromagnetic field.[85,86] AgNPs, in particular, exhibit an exceptionally strong localised SPR effect due to their unique electron confinement properties, as highlighted by.[86] This distinctive characteristic allows for their precise detection. AgNPs are known to display distinctive absorbance peaks within the 380–450 nm range, a feature contingent on their size and shapes, as demonstrated by various studies such as.[87–89] For the analysis, following a 3 hours synthesis period, the AgNP samples were scanned between 300 and 500 nm, as illustrated in Fig. 4. Table 1 presents the maximum absorbance (λ_{max}) values for each sample. The experiments were conducted with various synthesis times to identify the minimum reaction time required for the suc-
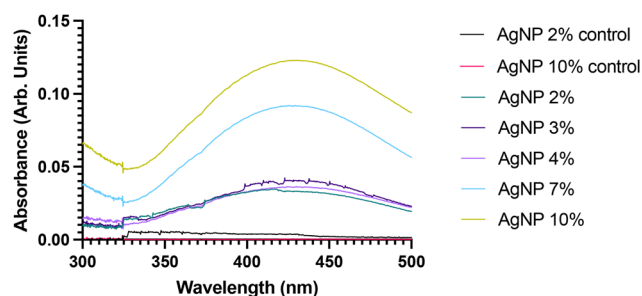
Fig. 4 UV-Visible spectra of synthesised AgNPs following 3 hours of synthesis period for the different *S. oleracea* leaf extract concentrations (AgNP 0%, AgNP-2%, AgNP-3%, AgNP-4%, AgNP-7% and 10%). Results show the absence of spectral absorbance curves in the control samples for both the 2% control and 10% control *S. oleracea* leaf extract control concentrations.
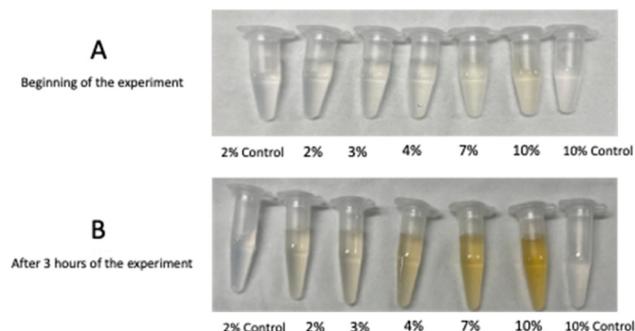
Fig. 3 Visual confirmation of the synthesis of the AgNPs through a colour change from light green (A) to yellowish brown (B). Pictures show the five concentrations AgNP 2%, AgNP 3%, AgNP 4%, AgNP 7% and AgNP 10%, as well as controls for AgNP 2% and AgNP 10%. Controls have no *S. oleracea* leaf extract.

Table 1 Maximum absorbance peaks (λ_{max}) of the SPR band of the synthesised AgNP samples AgNP-2%, AgNP-3%, AgNP-4%, AgNP-7% and AgNP-10%

Sample (% *S. oleracea* leaf extract)	λ_{max}	Absorbance
AgNP-2%	415–417 nm	0.0347
AgNP-3%	423 nm	0.0424
AgNP-4%	425 nm	0.0917
AgNP-7%	428 nm	0.0920
AgNP-10%	445 nm	0.1207

cessful synthesis of AgNPs. The results confirmed the presence of AgNPs in all samples, as evidenced by absorbance curves present in all AgNP concentrations ranging from 390–500 nm. Notably, distinct absorbance peaks were observed in the 415–445 nm range. Furthermore, an interesting observation was made regarding the impact of *S. oleracea* leaf extract concentration. An increase in extract concentration correlated with higher absorbances in the spectral bands. For instance, AgNP 10% exhibited the highest absorbance at 0.1207, while AgNP-2% displayed an absorbance of 0.0347.

Nanoparticle shape determination using SEM

SEM offers a valuable tool for assessing the morphological characteristics of the synthesised AgNPs. It measures the scattering of a high energy beam of electrons within the sample.[90] By analysing these scattered signals, SEM provides valuable insights into particles' surface topography, including their size and shape.[90] Consequently, SEM was employed to investigate the morphology of the synthesised AgNPs. The reference literature for this study, by using *Amaranthus Tricolor* L. (red spinach), similar leaf extract concentration, as well as the baseline methodology, obtained spherical nanoparticles.[37] As such, a spherical shape was anticipated for our synthesised AgNPs; however, it is worth noting that updates to the experimental methods and optimisations may impact this outcome. Fig. 5 presents the outcomes of the SEM analysis, revealing the predominantly spherical shape of the synthesised AgNPs. Notably, it was observed that at lower *S. oleracea* leaf extract concentrations (AgNPs 2% – 189 nm and AgNPs 3% – 154 nm),

the AgNPs tend to aggregate, resulting in a slightly larger average diameter. In contrast, at higher *S. oleracea* leaf extract concentrations (AgNPs 4% – 106 nm, AgNPs 7% – 142 nm, and AgNPs 10% – 127 nm), AgNPs exhibited less aggregation. Hence resulting in a lower AgNP size. The SEM measurements indicated that the AgNPs appeared somewhat larger in size compared to the results obtained from DLS analysis, with the exception of AgNPs 2%, which remained relatively consistent. Overall, the SEM results demonstrated improved monodispersity and a more evenly distributed.

Nanoparticle size determination using DLS

The morphological assessment of the size and size distribution of the AgNPs were analysed using a Malvern Nanosizer DLS machine. DLS measures the scattering (direction and intensity of light) of particles in a liquid medium when exposed to an electromagnetic wave and uses the diffusion coefficient to report the hydrodynamic size and size distribution.[91,92] Additionally, the size distribution provides information on the dispersity of the population of AgNPs represented by the Polydispersity Index (PDI) values.[92] In drug delivery research, it is typically considered acceptable for PDI values to fall within the range of 0.1 to 0.4, as reported by Sharma *et al.* in 2014.[93] Table 2 showcases the resulting data on average particle size and PDI values for each of the samples. The data revealed a bidirectional correlation between *S. oleracea* leaf extract concentration and AgNP size. In the case of lower *S. oleracea* leaf extract concentrations, specifically AgNP-2% (173 nm) and AgNP-3% (311 nm), an increase in par-
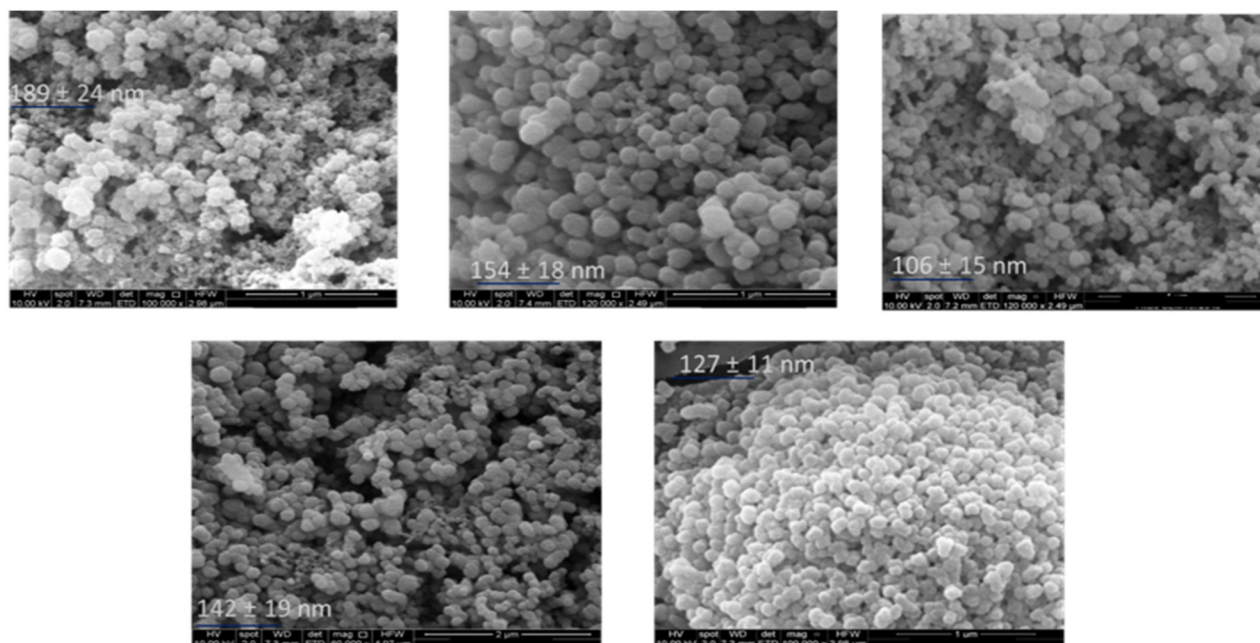
Fig. 5 SEM analysis result of synthesised AgNPs shows the synthesised AgNPs revealing the different shapes and sizes of the synthesised particles: (a) AgNP 2% – 189 ± 24 nm, (b) AgNP 3% – 154 ± 18 nm, (c) AgNP 4% – 106 ± 15 nm, (d) AgNP 7% – 142 ± 19 nm and (e) AgNP 10% – 127 ± 11nm, from top left to bottom right. Results show all the samples presenting spherically shaped nanoparticles. Results also show aggregations and slightly larger particle size in the lower *S. oleracea* leaf extract concentrations AgNP 2% (189 nm) and AgNP 3% (154 nm), compared to the higher concentrations (AgNP 4% 106 nm, AgNP 7% 142 nm and AgNP 10% 127 nm).

Table 2 DLS analysis result of *S. oleracea* leaf extract mediated AgNPs with concentrations of AgNP-2%, AgNP-3%, AgNP-4%, AgNP-7% and AgNP-10%. Analytical data indicates the formation of particles with sizes ranging from 109 nm to 211 nm. Notably, the data exhibits a distinct pattern: an increase in the average particle size is observed in samples with lower concentrations of *S. oleracea* leaf extract, specifically AgNP-2% and AgNP-3%. Conversely, a trend of size reduction is evident in the AgNP samples with higher concentrations, namely AgNP-4%, AgNP-7% and AgNP-10%. It is noteworthy that all of the synthesised AgNPs exhibited PDI values below the threshold of 0.5, signifying a good degree of uniformity within the particle population.

S. oleracea leaf extract (%)	*Z*-Average (nm)	PDI
AgNP-2%	173 ± 14.6	0.2 ± 0.02
AgNP-3%	211 ± 66.4	0.4 ± 0.09
AgNP-4%	148 ± 21.6	0.2 ± 0.06
AgNP-7%	120 ± 8.6	0.2 ± 0.04
AgNP-10%	109 ± 4.3	0.3 ± 0.02

ticle size occurred. Conversely, a further increase in *S. oleracea* leaf extract concentration led to reductions in size within the higher concentration AgNPs: AgNP-4% (148 nm), AgNP-7% (120 nm), and AgNP-10% (109 nm). As such, the highest phytochemical concentration particle resulted in the lowest particle, revealing the enhanced stabilisation effects of the higher phytochemical concentration resulting in particle size reductions.

Remarkably, all the synthesised AgNPs exhibited PDI values below 0.5, signifying a good level of monodispersion within the sample population, aligning with the findings discussed by other studies.[94]

Nanoparticle chemical properties analysis using ATR-FTIR

ATR-FTIR (Attenuated Total Reflectance Fourier-Transform Infrared) spectroscopy is a technique used to generate spectra showing the transmission or absorbance of specific functional groups and chemical bonds within samples.[95,96] In our study, ATR-FTIR was employed to verify the presence of distinct plant-associated functional groups and biomolecules such as –OH, –COOH, and –NH within the samples, indicating the effective binding, reduction, and stabilisation of the AgNPs by *S. oleracea* leaf extract.[84] Fig. 6 shows the results of the ATR-FTIR analysis of the synthesised AgNP and *S. oleracea* leaf extract, along with the observed spectral stretches. Each of these stretches corresponds to the presence and absorbance of specific functional groups associated with *S. oleracea* leaf extract and the synthesised AgNPs. The ATR-FTIR analysis involved comparing the spectra of each of the synthesised AgNPs to the spectrum of *S. oleracea* leaf extract. Remarkably, the results and band stretches were consistent across all the AgNP samples. The ATR-FTIR spectra of *S. oleracea* leaf extract exhibited peaks at approximately 3128 cm⁻¹, 2836 cm⁻¹,
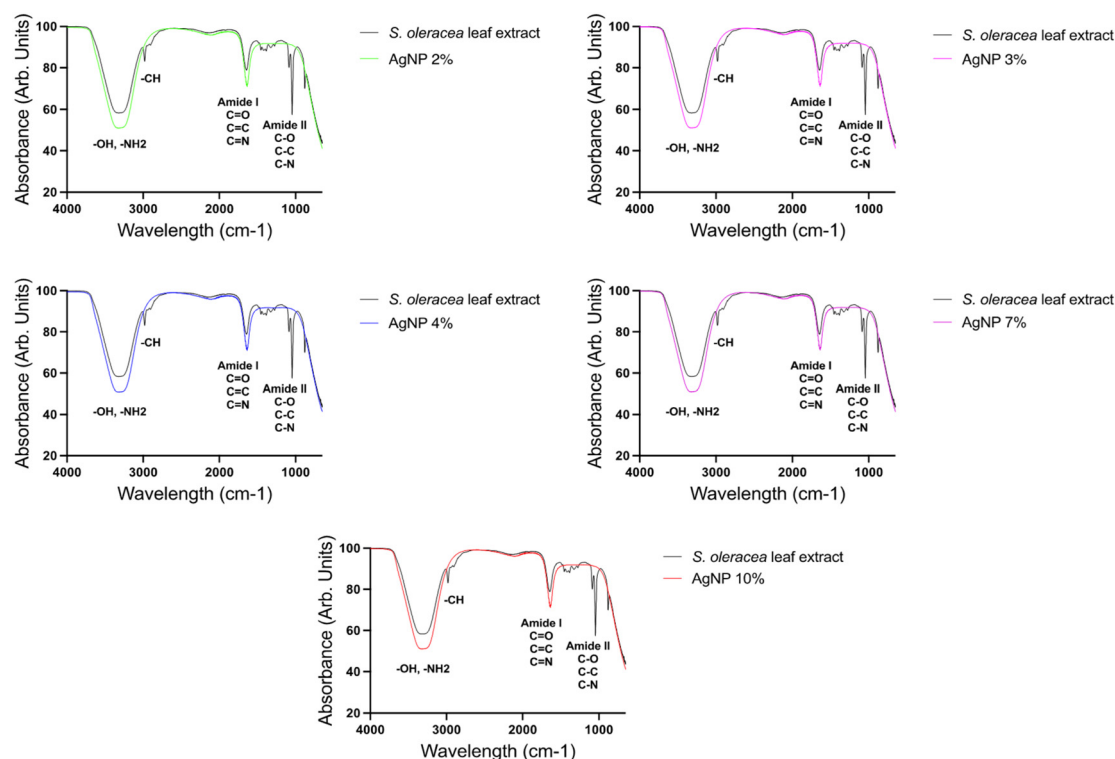
Fig. 6 ATR-FTIR analysis result showing the percentage of infrared light transmitted for different functional groups and bonds located on the spectrum. The analysis was conducted for all five concentrations of AgNP 2%, AgNP 3%, AgNP 4%, AgNP 7% and AgNP 10% and compared with *S. oleracea* leaf extract. The spectral stretches observed for each of the synthesised concentrations were found to be in similar locations as the labelled peaks in the *S. oleracea* leaf extract spectrum. These results indicate the presence of plant biomolecule functional groups in all concentrations of the synthesised AgNPs.

$1642 \ cm^{-1}$, and $1042 \ cm^{-1}$. Following the AgNP synthesis process shifts in these peaks were observed, though they remained in the same area generally. Specifically, the results showed peaks in *S. oleracea* leaf extract at $3128 \ cm^{-1}$, $1642 \ cm^{-1}$, and $1042 \ cm^{-1}$ shifted to $3153 \ cm^{-1}$, $1651 \ cm^{-1}$, and $1050 \ cm^{-1}$ in the synthesised AgNPs. Notably, the disappearance of the peak at $2836 \ cm^{-1}$ indicates the bioreduction of Ag^+ to Ag^0, as previously noted in other studies.[84,97] These observed changes, including shifts and the disappearance of peaks, provide evidence of the involvement of plant functional groups in the binding mechanisms that facilitate the synthesis of AgNPs. Furthermore, the prominent band stretch around $3151 \ cm^{-1}$ in both *S. oleracea* leaf extract and the AgNPs suggests the presence of amino acids, resulting in stretching vibrations of the O–H hydroxy group.[98,99] The peaks at $2836 \ cm^{-1}$, $2183 \ cm^{-1}$, and $2146 \ cm^{-1}$ are indicative of the stretching of aliphatic groups, attributed to plant chlorophyll (Kohan Baghkheirati *et al.*, 2016; Ramamurthy & Kannan, 2007). The stretching vibrations of carbonyl groups (–C=O, –C=C, –C=N) can also be observed through the bands at $1642 \ cm^{-1}$ and $1651 \ cm^{-1}$, signifying the presence of secondary amides present in proteins (Ramamurthy & Kannan, 2007). It is worth noting that these double bond chain groups (C=O, –C=C, and C=N) are more pronounced in the synthesised AgNPs compared to the extract-only spectra, providing further evidence of double bond formation and effective stabilisation of AgNPs, as depicted in Fig. 8. Finally, the observed peaks at

$1042 \ cm^{-1}$ and $1050 \ cm^{-1}$ are characterised by the stretching of aliphatic amines.[97]

Nanoparticle elemental composition using ICP-QMS

The elemental composition of various concentrations of AgNPs was assessed using ICP-QMS, a powerful analytical technique capable of quantifying trace elements and isotopic concentrations in diverse samples.[100–102] *S. oleracea* leaf extract is known to be rich in minerals such as Potassium (K), Copper (Cu), Calcium (Ca), Iron (Fe), Zinc (Zn) and Manganese (Mn).[103,104] Hence, the presence of these elements in the fabricated AgNPs may indicate their effective reduction and stabilisation by the plant material. To investigate this, the analysis compared the concentrations ($\mu g \ L^{-1}$) of elements in the synthesised AgNPs with those in *S. oleracea* leaf extract alone. The analytical results are depicted in graphs 7a, 7b and 7c.

The analysis revealed the detection of various elements, but elements present in very minimal amounts were excluded from consideration. The graphs represent elements that were detected at significant concentration levels. Specifically, elemental ions such as potassium ions, calcium ions, iron ions, chromium ions, nickel ions, copper ions, cobalt ions and Ag ions were present at substantial concentration levels ranging from as low as $0.25 \ \mu g \ L^{-1}$ to as high as $198 \ 500 \ \mu g \ L^{-1}$ in both the extract and AgNP samples. In considerably higher concentrations, the *S. oleracea* leaf extract sample exhibited elements including potassium ions, Ag ions, calcium ions,
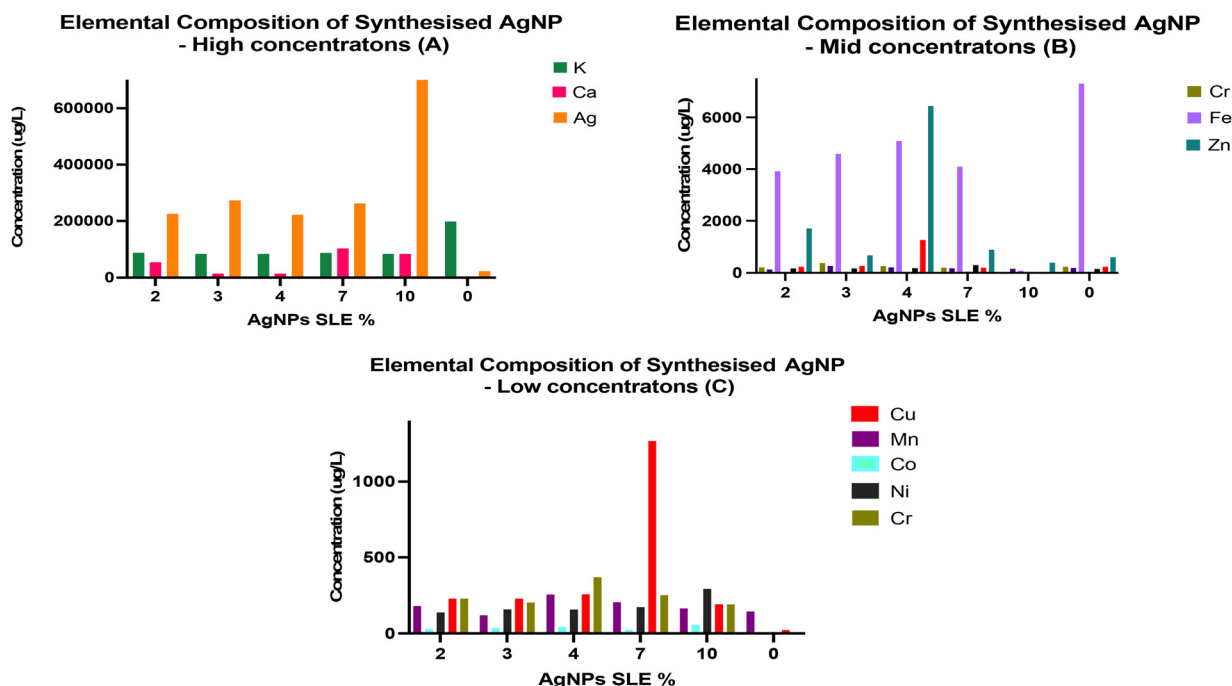

Fig. 7 (A, B and C), shows the metallomics analysis result of the synthesised AgNPs (2%, 3%, 4%, 7% and 10%), with 0 representing the *S. oleracea* leaf extract alone. They reveal the elemental composition of the synthesised AgNPs. The elemental composition is shown in order of highest (A) to mid (B) to lower (C) concentrations. All the synthesised AgNPs had considerable amounts of Ag ions as can be seen, with the highest occurring in AgNP-10%. The analysis also showed the presence of essential *S. oleracea* leaf extract related elements in all the synthesised AgNPs, including Potassium ions, Copper ions, Iron ions, Chromium ions, Zinc ions and Manganese ions.
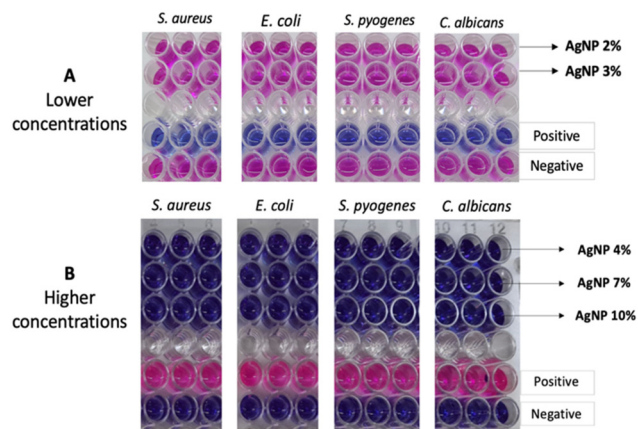
Fig. 8 (A) and (B) illustrates the antimicrobial activity evaluation of the generated AgNPs against *S. aureus*, *E. coli*, *S. pyogenes* and *C. albicans*. The lower concentration AgNPs did not exhibit any inhibitory activity against the microbes, as indicated by the colour change to pink due to metabolic activity. Conversely, all the higher *S. oleracea* leaf extract concentration AgNPs (Shown in 8B), achieved full inhibition of all tested microbes, evidenced by the lack of colour change due to the absence of metabolic activity.

and zinc ions. The samples also contained trace amounts of manganese ions, iron ions, copper ions, chromium ions, nickel ions and cobalt ions. Similarly, these elements were present all the *S. oleracea* leaf extract mediated AgNPs, although in varying quantities. The concentration of potassium ions in the samples was highest overall, with its quantities observed to slightly decrease with increasing *S. oleracea* leaf extract and phytochemical concentration in the AgNPs. Next, significantly higher amounts of calcium ions was found to be present in the AgNP samples compared to *S. oleracea* leaf extract on its own. Notably, the highest concentration AgNPs (AgNP-7% and AgNP-10%), had the highest amount of calcium ions compared to the lower concentrations (AgNP-2%, AgNP-3% and AgNP-4%). Furthermore, the concentration of zinc ions in the *S. oleracea* leaf extract was found to be considerably lower than the amounts in the synthesised AgNPs. Herein, the AgNP-2% had the highest iron ions amount of 7298 µg L^{-1}; however, there was a general decrease in the other AgNP concentrations. Similarly, the amounts of nickel ions in the *S. oleracea* leaf extract alone sample were trace levels. However, significantly more were present in the AgNP sample, with an increase in concentration observed with increased extract concentration. Lastly, some levels of Ag ions were found in the *S. oleracea* leaf extract, which has been reported by other studies.[105] However, significantly more was identified in the AgNP samples. Notably, a general increase in Ag concentration was found from the lower extract AgNPs to the higher extract AgNPs, with the AgNP-10% having the highest concentration of Ag ions (704, 595 µg L^{-1}). Notably these higher Ag ion content AgNPs, especially AgNP-10%, also had the highest phytochemical content. As such, the enhanced phytochemical content may have equally enhanced the potential of Ag generation in the sample.

Nanoparticle antimicrobial activity using the resazurin assay

Resazurin is a redox-sensitive dye utilised to assess cellular viability in various cytotoxicity and antimicrobial activity assays.[81] This assay operates on the principle that metabolically active living cells reduce non-fluorescent blue resazurin to fluorescent pink resorufin.[82] The observed colour change, and fluorescence signify microbial cell viability. Freshly cultured and diluted bacteria and fungi were exposed to different AgNP concentrations at two distinct ranges: lower (AgNPs-2% and AgNPs-3%) and higher (AgNPs-4%, AgNPs-7%, and AgNPs-10%). Previous research indicated that *S. oleracea* leaf extract lacks antimicrobial activity against *E. coli, S. aureus*, and *C. albicans*.[84] The effects of treating microorganisms with the synthesised AgNPs are displayed in Fig. 8A (lower concentration) and 8B (higher concentration). The results show that all lower concentration AgNPs had no inhibitory effect on *S. aureus, E. coli, S. pyogenes, and C. albicans*. In contrast, higher concentrations of *S. oleracea* extract AgNPs (AgNP-4%, AgNP-7%, and AgNP-10%) exhibited full bactericidal effects against all tested microbes, suggesting that higher concentrations of *S. oleracea* leaf extract enhances AgNP antimicrobial activity.

Discussion

Utilising plant-mediated synthesis for the development of metallic nanoparticles has been demonstrated as an environmentally friendly, cost-effective, and biocompatible approach to producing stable nanoparticles with promising therapeutic potential. In this investigation, spherical nanoscale AgNPs were successfully synthesised by using *S. oleracea* leaf extract and AgNO$_3$ as the source of Ag ions. The presence and effective formation of AgNPs was confirmed after the synthesis by observing a change in the initial sample colour from light green to yellowish brown (Fig. 3). Regarding morphological assessment, monodispersed AgNPs with sizes ranging from 109 nm to 211 nm were revealed using DLS (Table 2). Similarly, spherical particles with sizes ranging from 106 nm to 189 nm were confirmed in the SEM analysis of the AgNPs (Fig. 5). Additionally, the presence of functional groups and bond stretches associated with the *S. oleracea* leaf extract in the synthesised AgNPs was confirmed using ATR-FTIR (Fig. 6), highlighting the involvement of these plant-related components in the synthesis and stabilisation of AgNPs. Further assessment of the elemental composition of the AgNPs through ICP-QMS (Fig. 7) revealed the presence of elements related to *S. oleracea* leaf extract, including sodium ions, magnesium ions, silicon ions, potassium ions, calcium ions, and iron ions, alongside the core metal, Ag ions.

As a relatively new research field, the influence of the plant extract on the physiochemical properties of plant-mediated AgNPs remains unclear due to mixed findings in existing literature. The reduction of Ag ions and AgNP formation were monitored both visually and spectrophotometrically, with visual confirmation of AgNP formation occurring through a

colour change to yellowish brown (Fig. 3), a phenomenon reported in similar studies.[106,107] To further confirm the presence of AgNPs, UV-vis spectroscopy was conducted, as metallic nanoparticles like AgNPs absorb UV-visible light at specific wavelengths. Strong spectral absorbances in the range of 390 nm to 500 nm, with peaks typically around 415 nm to 445 nm, depending on *S. oleracea* leaf extract concentration (Fig. 4), were revealed in the analysis. This finding is consistent with similar plant-mediated AgNP synthesis studies.[106,108] The SEM morphological assessment of the AgNPs indicated spherical particle shapes, with significant aggregation within the particle population observed in lower concentrations of *S. oleracea* leaf extract (AgNP-2% and AgNP-3%) (Fig. 5). This aggregation tendency in lower concentrations may be attributed to reduced amounts of phytochemicals from the *S. oleracea* leaf extract in the reaction medium, which prolonged the growth phase has it reduced the stabilisation potential and particle size control of those nanoparticles. This probable phenomenon aligns with reports in similar studies.[31,109] Moreover, the DLS analysis also supported these findings, revealing an inverse relationship between particle size and plant material concentration (Table 2). Herein, AgNPs with the highest concentration of *S. oleracea* leaf extract and phytochemical content had the lowest sizes, and AgNPs with the lowest concentration of *S. oleracea* leaf extract had the highest size. Again, this establishes the major role phytochemicals play in particle stabilisation and size control. These results are interesting because there have been conflicting reports regarding the impact of plant extracts on the size of AgNPs, with certain studies proposing that higher concentrations result in larger particles, while others offer a contrasting perspective. In metallic nanoparticle synthesis, two critical phases are involved: the reduction and growth/stabilisation phases.[110] The latter is necessary for maintaining stability at the interface between the ionic particles and the nanoparticle synthesis medium. In plant-mediated synthesis, phytochemicals within the organic material serve as both reducing and stabilising agents, creating a biological corona around the particles.[110] Hence, sufficient amounts of plant material and phytochemicals are required to prevent aggregation and the formation of larger particles, explaining the observed trend of larger particles in lower *S. oleracea* leaf extract concentrations and smaller particles in higher concentrations. As such, this study highlights the correlation between AgNP size and extract concentration in dictating that adequate amounts of the stabilisation compounds within phytochemicals are necessary for the production of smaller AgNPs. Notably, more reduction in particle size was observed in AgNP-10% compared to AgNP-2%

The stabilisation capacity of *S. oleracea* leaf extract was validated through ATR-FTIR analysis by the presence of phytochemical related functional groups and biochemicals (*e.g.* OH, COOH) (Fig. 6). These findings align with previous studies, establishing the significance of these functional groups as essential contributors to the stabilisation and nanoparticle generation process.[111,112] These functional groups associated with *S. oleracea* leaf extract phytochemicals were also detected in the synthesised AgNPs, providing clear evidence of their reduction and stabilisation by the phytochemicals in the extract. Lastly, *S. oleracea* leaf extract has been shown to possess elements such as sodium, iron, potassium, calcium, silicon, and magnesium.[113,114] The presence of these elemental ions in all the synthesised AgNPs may suggest their effective interaction with plant extract (Fig. 7). Interestingly, there were higher amounts of Ag ions in the AgNP-10% sample and lower amounts of Ag ions in the AgNP-2% (Fig. 7A). Studies have shown that the therapeutic effect, including the antibacterial activity of AgNPs, depends on the concentration and amount of Ag ions released.[115,116] Thus, the presence of more Ag ions in AgNP-10% may confer an increased potential for Ag ion related bactericidal activity. This also highlights the role of phytochemical concentration in improving antibacterial capacity by facilitating the generation of more Ag ions in AgNPs.

Turning to the antimicrobial activity of the generated AgNPs, the lower concentration AgNPs showed no antimicrobial activity (Fig. 8A). In contrast, the higher concentration AgNPs, *i.e.* those with slightly higher *S. oleracea* leaf extract contents, fully inhibited all tested microbes: *E. coli*, *S. aureus*, *S. pyogenes* and *C. albicans* (Fig. 8B). Therefore, this shows the potential of higher extract content to facilitate increased antimicrobial activity, which may be due to increased Ag generation as shown in the ICPQMS elemental analysis. While previous studies have reported greater bactericidal effects of AgNPs on Gram-negative bacteria due to membrane interactions, results obtained here demonstrate high concentration *S. oleracea* leaf extract mediated AgNPs can inhibit both, indicating their potential as broad-spectrum antimicrobial agents.[117–119] This corroborates findings from Loo *et al.*, 2018,[120] as they also observed potent antimicrobial effects of plant-mediated AgNPs on both bacterial types. Moreover, this broad-spectrum efficacy is particularly advantageous for the potential of tackling infections caused by stubborn bacteria such as *M. TB*, which pose a significant global health burden.[121] Furthermore, the higher *S. oleracea* leaf extract concentrations were also effective against fungi *C. albicans*, highlighting their effectiveness against resilient fungal cells. This finding is particularly significant because, generally, fungal cells are known to be tough targets for reasons including their tough cell walls that impede penetration of antifungal agents.[122,123] *C. albicans* is a major pathogen responsible for life threatening fungal infections globally.[63,124] The anti- *C. albicans* activity due to the *S. oleracea* leaf extract mediated AgNPs observed may be due to mechanisms including ROS generation and fungal cell membrane disruptions.[125,126] Studies have also shown these effects are also size dependent, with smaller particles exhibiting increased antifungal properties due to their larger surface area.[127,128] This may explain the lack of antifungal activity in the larger AgNPs (AgNP-2% and AgNP-3%), synthesised with lower concentrations of *S. oleracea* leaf extract and lower phytochemical content.

Conclusion

In conclusion, plant mediated AgNPs were successfully synthesised using different concentrations of *S. oleracea* leaf extract. The complete absence of toxic chemicals and additives in this process emphasises its potential to drive nanoparticle development towards sustainable, biocompatible, and cost-effective practices. Our investigation revealed the synthesis of nanosized *S. oleracea* leaf extract mediated AgNPs is substantially influenced by the extract concentration. Notably, higher extract concentrations yielded smaller and more monodispersed AgNPs, highlighting the pivotal role of extract concentration in determining the morphological properties of AgNPs. These findings challenge some earlier reports and emphasise the critical need for precise control over synthesis parameters in plant mediated AgNP production. Moreover, the antimicrobial assays highlighted the good spectrum activity of AgNPs synthesised with higher *S. oleracea* leaf extract concentrations. They all had remarkable activity against fungi as well as Gram positive and Gram negative bacteria through full inhibition of *E. coli*, *S. aureus*, *S. pyogenes* and *C. albicans*. These findings gain substantial significance in the face of escalating antibiotic resistance among pathogens, thus revealing biologically developed AgNPs as promising alternatives for combating antibacterial drug resistance issues.

Author contributions

Tamara Akpobolokemi: conceptualization, methodology, investigation, writing – original draft. Etelka Chung: methodology, investigation, writing – review & editing. Rocio Teresa Martinez-Nunez: resources, writing – review & editing, supervision. Guogang Ren: resources, writing – review & editing. Alex Griffiths: methodology, investigation, writing – review & editing, Bahijja Tolulope Raimi Abraham: conceptualization, resources, writing – review & editing, supervision. All authors have given approval to the final version of the manuscript.

Data availability

All the data presented in this paper are available from the authors.

Conflicts of interest

There are no conflicts to declare.

Acknowledgements

References

1 M. Kerker, The optics of colloidal silver: something old and something new, *J. Colloid Interface Sci.*, 1985, **105**(2), 20–25.

2 K. Anand, K. Kaviyarasu, S. Muniyasamy, S. M. Roopan, R. M. Gengan and A. A. Chuturgoon, Bio-Synthesis of Silver Nanoparticles Using Agroforestry Residue and Their Catalytic Degradation for Sustainable Waste Management, *J. Cluster Sci.*, 2017, **28**(4), 2279–2291.

3 B. Kar, D. Pradhan, P. Mishra, S. K. Bhuyan, G. Ghosh and G. Rath, Exploring the Potential of Metal Nanoparticles as a Possible Therapeutic Adjunct for Covid-19 Infection, *Proc. Natl. Acad. Sci., India, Sect. B*, 2022, **92**(3), 511–521, **https://link.springer.com/article/10.1007/s40011-022-01371-1**.

4 J. J. Xu, W. C. Zhang, Y. W. Guo, X. Y. Chen and Y. N. Zhang, Metal nanoparticles as a promising technology in targeted cancer treatment, *Drug Delivery*, 2022, **29**(1), 664–678, **https://www.tandfonline.com/doi/abs/10.1080/10717544.2022.2039804**.

5 R. Vishwanath and B. Negi, Conventional and green methods of synthesis of silver nanoparticles and their antimicrobial properties, *Curr. Res. Green Sustainable Chem.*, 2021, **4**, 2–4.

6 B. Bhardwaj, P. Singh, A. Kumar, S. Kumar and V. Budhwar, Eco-Friendly Greener Synthesis of Nanoparticles, *Adv. Pharm. Bull.*, 2020, **10**(4), 566, **https://pmc/articles/PMC7539319/**.

7 H. Chandra, P. Kumari, E. Bontempi and S. Yadav, Medicinal plants: Treasure trove for green synthesis of metallic nanoparticles and their biomedical applications, *Biocatal. Agric. Biotechnol.*, 2020, **24**, 2–4.

8 A. M. El Shafey, Green synthesis of metal and metal oxide nanoparticles from plant leaf extracts and their applications: A review, *Green Process. Synth.*, 2020, **9**(1), 304–339, **https://www.degruyter.com/document/doi/10.1515/gps-2020-0031/html**.

9 K. N. Ganesh, D. Zhang, S. J. Miller, K. Rossen, P. J. Chirik, M. C. Kozlowski, *et al.*, Green Chemistry: A Framework for a Sustainable Future, *Org. Process Res. Dev.*, 2021, **25**, 1801–1805.

10 A. Chakravarty, I. Ahmad, P. Singh, M. U. D. Sheikh, G. Aalam, S. Sagadevan, *et al.*, Green synthesis of silver nanoparticles using fruits extracts of Syzygium cumini and their bioactivity, *Chem. Phys. Lett.*, 2022, **795**, 2–5.

11 J. Pei, B. Fu, L. Jiang and T. Sun, Biosynthesis, characterization, and anticancer effect of plant-mediated silver nano-

particles using Coptis chinensis, *Int. J. Nanomed.*, 2019, **14**, 1969–1978.

12 M. Baláž, Ľ. Balážová, N. Daneu, E. Dutková, M. Balážová, Z. Bujňáková, *et al.*, Plant-Mediated Synthesis of Silver Nanoparticles and Their Stabilization by Wet Stirred Media Milling, *Nanoscale Res. Lett.*, 2017, **12**(1), 83, DOI: **10.1186/s11671-017-1860-z**.

13 M. Gholami-Shabani, F. Sotoodehnejadnematalahi, M. Shams-Ghahfarokhi, A. Eslamifar and M. Razzaghi-Abyaneh, Physicochemical properties, anticancer and antimicrobial activities of metallic nanoparticles green synthesized by Aspergillus kambarensis, *IET Nanobiotechnol.*, 2022, **16**(1), 1–13, **https://onlinelibrary.wiley.com/doi/full/10.1049/nbt2.12070**.

14 S. Shivaji, S. Madhu and S. Singh, Extracellular synthesis of antibacterial silver nanoparticles using psychrophilic bacteria, *Process Biochem.*, 2011, **46**(9), 2–3.

15 P. Shivakrishna, R. Prasad, G. Krishna and S. Charya, Synthesis of Silver Nano Particles from Marine Bacteria Pseudomonas aerogenosa, *Octa J. Biosci.*, 2013, **1**(2), 2–4.

16 M. Ovais, A. T. Khalil, N. U. Islam, I. Ahmad, M. Ayaz, M. Saravanan, *et al.*, Role of plant phytochemicals and microbial enzymes in biosynthesis of metallic nanoparticles, *Appl. Microbiol. Biotechnol.*, 2018, **102**, 6800–6809.

17 S. Yallappa and J. Manjanna, Biological Evaluation of Silver Nanoparticles Obtained from T. arjuna Bark Extract as Both Reducing and Capping Agent, *J. Cluster Sci.*, 2014, **25**(5), 1450–1461.

18 S. K. Nune, N. Chanda, R. Shukla, K. Katti, R. R. Kulkarni, S. Thilakavathy, *et al.*, Green nanotechnology from tea: phytochemicals in tea as building blocks for production of biocompatible gold nanoparticles, *J. Mater. Chem.*, 2009, **19**(19), 2912–2920, **https://pubs.rsc.org/en/content/articlehtml/2009/jm/b822015h**.

19 D. Martínez-Bernett, A. Silva-Granados, S. N. Correa-Torres and A. Herrera, Chromatographic analysis of phytochemicals components present in mangifera indica leaves for the synthesis of silver nanoparticles by AgNO3 reduction, *J. Phys.:Conf. Ser.*, 2016, **687**(1), 1–4, **https://iopscience.iop.org/article/10.1088/1742-6596/687/1/012033**.

20 Z. Yousaf and N. Saleh. *Advanced Concept of Green Synthesis of Metallic Nanoparticles by Reducing Phytochemicals*. 2018, pp. 17–36. **https://link.springer.com/chapter/10.1007/978-3-319-77119-9_2**.

21 I. Shaheen and K. S. Ahmad, Chromatographic identification of "green capping agents" extracted from Nasturtium officinale (Brassicaceae) leaves for the synthesis of MoO3 nanoparticles, *J. Sep. Sci.*, 2020, **43**(3), 598–605.

22 W. J. Aziz, M. A. Abid and E. H. Hussein, Biosynthesis of CuO nanoparticles and synergistic antibacterial activity using mint leaf extract, *Mater. Technol.*, 2020, **35**(8), 447–451, **https://www.tandfonline.com/doi/abs/10.1080/10667857.2019.1692163**.

23 A. I. Felimban, N. S. Alharbi and N. S. Alsubhi, Optimization, Characterization, and Anticancer Potential of Silver Nanoparticles Biosynthesized Using Olea europaea, *Int. J. Biomater.*, 2022, **2022**, 1–10.

24 A. Miranda, T. Akpobolokemi, E. Chung, G. Ren and B. T. Raimi Abraham, pH Alteration in Plant-Mediated Green Synthesis and Its Resultant Impact on Antimicrobial Properties of Silver Nanoparticles (AgNPs), *Antibiotics*, 2022, **11**(11), 1–15, **https://www.mdpi.com/2079-6382/11/11/1592**.

25 A. K. Sidhu, N. Verma and P. Kaushal, Role of Biogenic Capping Agents in the Synthesis of Metallic Nanoparticles and Evaluation of Their Therapeutic Potential, *Front. Nanotechnol.*, 2022, **3**, 105.

26 J. M. Ashraf, M. A. Ansari, H. M. Khan, M. A. Alzohairy and I. Choi, Green synthesis of silver nanoparticles and characterization of their inhibitory effects on AGEs formation using biophysical techniques, *Sci. Rep.*, 2016, **6**, 1–10.

27 H. Liu, H. Zhang, J. Wang and J. Wei, Effect of temperature on the size of biosynthesized silver nanoparticle: Deep insight into microscopic kinetics analysis, *Arabian J. Chem.*, 2020, **13**(1), 1012–1017.

28 S. Iravani and B. Zolfaghari, Green synthesis of silver nanoparticles using Pinus eldarica bark extract, *BioMed Res. Int.*, 2013, **2013**, 1–4.

29 N. W. Mamdooh and G. A. Naeem, The effect of temperature on green synthesis of silver nanoparticles, *AIP Conf. Proc.*, 2022, **2450**(1), 2–5, **https://aip/acp/article/2450/1/020045/2824075/The-effect-of-temperature-on-green-synthesis-of**.

30 K. X. Lee, K. Shameli, S. E. Mohamad, Y. P. Yew, E. Dayana, M. Isa, *et al.*, Bio-mediated synthesis and characterisation of silver nanocarrier, and its potent anti-cancer action, *MDPI*, 2019, **9**(10), 14, **https://www.mdpi.com/2079-4991/9/10/1423**.

31 M. M. H. Khalil, E. H. Ismail, K. Z. El-Baghdady and D. Mohamed, Green synthesis of silver nanoparticles using olive leaf extract and its antibacterial activity, *Arabian J. Chem.*, 2014, **7**(6), 1131–1137.

32 N. Skandalis, A. Dimopoulou, A. Georgopoulou, N. Gallios, D. Papadopoulos, D. Tsipas, *et al.*, The effect of silver nanoparticles size, produced using plant extract from Arbutus unedo, on their antibacterial efficacy, *Nanomaterials*, 2017, **7**(7), 178.

33 J. Sun, F. Wang, Y. Sui, Z. She, W. Zhai, C. Wang, *et al.* Effect of particle size on solubility, dissolution rate, and oral bioavailability: evaluation using coenzyme Q_{10} as naked nanocrystals, *Int. J. Nanomed.*, 2012, **7**, 5733–5744, **https://www.ncbi.nlm.nih.gov/pubmed/23166438**.

34 L. Shang, K. Nienhaus, X. Jiang, L. Yang, K. Landfester, V. Mailänder, *et al.*, Nanoparticle interactions with live cells: Quantitative fluorescence microscopy of nanoparticle size effects, *Beilstein J. Nanotechnol.*, 2014, **5**(1), 2388–2397, **https://www.beilstein-journals.org/bjnano/articles/5/248**.

35 K. Sigfridsson, A. J. Lundqvist and M. Strimfors, Particle size reduction for improvement of oral absorption of the poorly soluble drug UG558 in rats during early development, *Drug Dev. Ind. Pharm.*, 2009, **35**(12), 1479–1486.

36 S. P. Ju, A molecular dynamics simulation of the adsorption of water molecules surrounding an Au nanoparticle, *J. Chem. Phys.*, 2005, **122**(9), 0947181–0947186.

37 I. Fatimah and Z. H. V. I. Aftrid, Characteristics and antibacterial activity of green synthesized silver nanoparticles using red spinach (Amaranthus Tricolor L.) leaf extract, *Green Chem. Lett. Rev.*, 2019, **12**, 25–29.

38 Z. Zarei, D. Razmjoue and J. Karimi, Green Synthesis of Silver Nanoparticles from Caralluma tuberculata Extract and its Antibacterial Activity, *J. Inorg. Organomet. Polym. Mater.*, 2020, **30**(11), 4606–4614.

39 M. R. Shaik, M. Khan, M. Kuniyil, A. Al-Warthan, H. Z. Alkhathlan, M. R. H. Siddiqui, *et al.*, Plant-Extract-Assisted green synthesis of silver nanoparticles using Origanum vulgare L. Extract and their microbicidal activities, *Sustainability*, 2018, **10**(4), 1–14.

40 B. Ajitha, Y. Ashok Kumar Reddy and P. Sreedhara Reddy, Green synthesis and characterization of silver nanoparticles using Lantana camara leaf extract, *Mater. Sci. Eng., C*, 2015, **49**, 373–381.

41 R. Revathy, J. Joseph, C. Augustine, T. Sajini and B. Mathew, Synthesis and catalytic applications of silver nanoparticles: a sustainable chemical approach using indigenous reducing and capping agents from Hyptis capitata, *Environ. Sci.:Adv.*, 2022, **1**(4), 491–505, **https://pubs.rsc.org/en/content/articlehtml/2022/va/d2va00044j**.

42 I. G. Antropova, A. A. Revina, P. M. Oo, E. S. Kurakina, I. A. Butorova and E. P. Magomedbekov, Synthesis of Silver Nanoparticles Using Reactive Water-Ethanol Extracts from Murraya paniculata, *ACS Omega*, 2021, **6**(12), 8313–8321, **https://pubs.acs.org/doi/full/10.1021/acsomega.1c00019**.

43 M. Khan, S. T. Khan, M. Khan, S. F. Adil, J. Musarrat, A. A. Al-Khedhairy, *et al.*, Antibacterial properties of silver nanoparticles synthesized using Pulicaria glutinosa plant extract as a green bioreductant, *Int. J. Nanomed.*, 2014, **9**(1), 3551–3565, **https://www.dovepress.com/antibacterial-properties-of-silver-nanoparticles-synthesized-using-pul-peer-reviewed-fulltext-article-IJN**.

44 A. Nejabatdoust, H. Zamani and A. Salehzadeh, Functionalization of ZnO Nanoparticles by Glutamic Acid and Conjugation with Thiosemicarbazide Alters Expression of Efflux Pump Genes in Multiple Drug-Resistant Staphylococcus aureus Strains, *Microb. Drug Resist.*, 2019, **25**(7), 966–974.

45 M. Abdolhosseini, H. Zamani and A. S. Biologia, *Synergistic antimicrobial potential of ciprofloxacin with silver nanoparticles conjugated to thiosemicarbazide against ciprofloxacin resistant Pseudomonas aeruginosa by*, Springer, 2019, pp. 1191–1196.

46 A. Murei, K. Pillay and A. Samie, Syntheses, Characterization, and Antibacterial Evaluation of P. grand-iflora Extracts Conjugated with Gold Nanoparticles, *J. Nanotechnol.*, 2021, **2021**, 1–9.

47 W. Jiang, W. Yang, X. Zhao, N. Wang and H. Ren, Klebsiella pneumoniae presents antimicrobial drug resistance for β-lactam through the ESBL/PBP signaling pathway, *Exp. Ther. Med.*, 2020, **19**(4), 2449, **https://pmc/articles/PMC7086219/**.

48 M. Franzolin, D. Courrol, F. Silva and L. C. Molecules, Antimicrobial Activity of Silver and Gold Nanoparticles Prepared by Photoreduction Process with Leaves and Fruit Extracts of Plinia cauliflora and Punica granatum, *Molecules*, 2022, **27**(20), 1–16, **https://www.mdpi.com/1882416**.

49 F. J. Osonga, A. Akgul, I. Yazgan, A. Akgul, G. B. Eshun, L. Sakhaee, *et al.*, Size and Shape-Dependent Antimicrobial Activities of Silver and Gold Nanoparticles: A Model Study as Potential Fungicides, *Molecules*, 2020, **25**(11), 2682, **https://pmc/articles/PMC7321160/?report=abstract**.

50 F. Fatima, P. Bajpai, N. Pathak, S. Singh, S. Priya and S. R. Verma, Antimicrobial and immunomodulatory efficacy of extracellularly synthesized silver and gold nanoparticles by a novel phosphate solubilizing fungus Bipolaris tetramera, *BMC Microbiol.*, 2015, **15**(1), 1–10, **https://bmcmicrobiol.biomedcentral.com/articles/10.1186/s12866-015-0391-y**.

51 S. Zhang, C. Du, Z. Wang, X. Han, K. Zhang and L. Liu, Reduced cytotoxicity of silver ions to mammalian cells at high concentration due to the formation of silver chloride, *Toxicol. in Vitro*, 2013, **27**(2), 739–744.

52 W. Sim, R. T. Barnard, M. A. T. Blaskovich and Z. M. Ziora, Antimicrobial silver in medicinal and consumer applications: A patent review of the past decade (2007–2017), *Antibiotics*, 2018, **7**, 1–15.

53 S. Staveski, C. Abrajano, M. Casazza, E. Bair, H. Quan, E. Dong, *et al.*, Silver-impregnated dressings for sternotomy incisions to prevent surgical site infections in children, *Am. J. Crit. Care*, 2016, **25**(5), 402–408.

54 L. M. Nherera, P. Trueman, C. D. Roberts and L. Berg, A systematic review and meta-analysis of clinical outcomes associated with nanocrystalline silver use compared to alternative silver delivery systems in the management of superficial and deep partial thickness burns, *Burns*, 2017, **43**(5), 939–948.

55 E. G. Haggag, A. M. Elshamy, M. A. Rabeh, N. M. Gabr, M. Salem, K. A. Youssif, *et al.*, Antiviral potential of green synthesized silver nanoparticles of lampranthus coccineus and malephora lutea, *Int. J. Nanomed.*, 2019, **14**, 6217–6229.

56 S. Gurunathan, J. W. Han, D. N. Kwon and J. H. Kim, Enhanced antibacterial and anti-biofilm activities of silver nanoparticles against Gram-negative and Gram-positive bacteria, *Nanoscale Res. Lett.*, 2014, **9**(1), 1–7.

57 K. Paulkumar, G. Gnanajobitha, M. Vanaja, S. Rajeshkumar, C. Malarkodi, K. Pandian, *et al.*, Piper nigrum leaf and stem assisted green synthesis of silver

nanoparticles and evaluation of its antibacterial activity against agricultural plant pathogens, *Sci. World J.*, 2014, **2014**, 1–8.

58 S. B. Aziz, G. Hussein, M. A. Brza, S. J. Mohammed, R. T. Abdulwahid, S. R. Saeed, *et al.*, Fabrication of Interconnected Plasmonic Spherical Silver Nanoparticles with Enhanced Localized Surface Plasmon Resonance (LSPR) Peaks Using Quince Leaf Extract Solution, *Nanomaterials*, 2019, **9**(11), 1557, https://pmc/articles/PMC6915396/.

59 A. D. Mare, A. Man, F. Toma, B. Tudor, L. Berța, C. Tanase, *et al.*, The antibacterial potential of biosynthe-sized silver nanoparticles using beech bark and spruce bark extracts, *Acta Marisiensis, Ser. Med.*, 2022, **68**(1), 17–23.

60 J. Osowicki, K. I. Azzopardi, L. Fabri, H. R. Frost, T. Rivera-Hernandez, M. R. Neeland, *et al.*, A controlled human infection model of Streptococcus pyogenes pharyngitis (CHIVAS-M75): an observational, dose-finding study, *Lancet Microbe*, 2021, **2**(7), 291–299, DOI: 10.1016/s2666-5247(20)30240-8.

61 M. Minami, R. Sakakibara, M. Watanabe and H. Morita, Analysis of Streptococcus pyogenes reinfection in pedi-atric patients in Japan, *GSC Adv. Res. Rev.*, 2021, **6**(3), 076–082, DOI: 10.30574/gscarr.2021.6.3.0045.

62 S. E. Bellamy, W. Ott, J. D. Kolb and K. Malik, A Complicated Clinical Course of Community-Acquired Staphylococcus aureus Infective Endocarditis, *Cureus*, 2023, 1–10, DOI: 10.7759/cureus.35973.

63 E. Ruiz-Baca, R. I. Arredondo-Sánchez, K. Corral-Pérez, A. Lopez-Rodriguez, I. Meneses-Morales, V. M. Ayala-García, *et al.*, Molecular Mechanisms of Resistance to Antifungals in Candida albicans, *Adv. Candida albicans*, 2021, 39–47, DOI: 10.5772/intechopen.96346.

64 R. A. A. Elshimy, Escherichia coli (E. coli) Resistance against Last Resort Antibiotics and Novel Approaches to Combat Antibiotic Resistance, *Escherichia Coli – Old and New Insights*, 2023, pp. 10–302. DOI: 10.5772/intechopen.104955.

65 C. K. Ezeh, C. N. Eze, M. E. U. Dibua and S. C. Emencheta, A meta-analysis on the prevalence of re-sistance of Staphylococcus aureus to different antibiotics in Nigeria, *Antimicrob. Resist. Infect. Control*, 2023, **12**(1), 1–22, DOI: 10.1186/s13756-023-01243-x.

66 H. M. Jasim, A. A. Farhan, H. R. Hassooni, A. Hassan and Alhusseiny, Detection of Tn916 Conferring Tetracycline Resistance in Clinical Isolates of Streptococcus pyogenes, *Indian J. Forensic Med. Toxicol.*, 2021, **15**(1), 2109–2113, DOI: 10.37506/ijfmt.v15i1.13717.

67 A. Abubakar and M. Haque, Preparation of medicinal plants: Basic extraction and fractionation procedures for experimental purposes, *J. Pharm. BioAllied Sci.*, 2020, **12**(1), 1–5.

68 E. J. Jeyaraj, Y. Y. Lim and W. S. Choo, Effect of Organic Solvents and Water Extraction on the Phytochemical Profile and Antioxidant Activity of Clitoria ternatea Flowers, *ACS Food Sci. Technol.*, 2021, **1**(9), 1567–1577, https://pubs.acs.org/doi/full/10.1021/acsfoodscitech.1c00168.

69 C. Y. Gan and A. A. Latiff, Optimisation of the solvent extraction of bioactive compounds from Parkia speciosa pod using response surface methodology, *Food Chem.*, 2011, **124**(3), 1277–1283.

70 A. W. Wahab, A. Karim, N. La Nafie, N. Nurafni and I. W. Sutapa, Synthesis of Silver Nanoparticles Using Muntingia Calabura L. Leaf Extract as Bioreductor and Applied as Glucose Nanosensor, *Orient. J. Chem.*, 2018, **34**(6), 3088–3094.

71 N. Liaqat, N. Jahan, T. Anwar and H. Qureshi, Green syn-thesized silver nanoparticles: Optimization, characteriz-ation, antimicrobial activity, and cytotoxicity study by hemolysis assay, *Front. Chem.*, 2022, **10**, 2–11, https://pmc/articles/PMC9465387/.

72 A. O. Dada, A. A. Inyinbor, E. I. Idu, O. M. Bello, A. P. Oluyori, T. A. Adelani-Akande, *et al.*, Effect of oper-ational parameters, characterization and antibacterial studies of green synthesis of silver nanoparticles using Tithonia diversifolia, *Peer J.*, 2018, **6**, 2–15, https://pmc/articles/PMC6214226/.

73 M. Darroudi, A. M. Bin, R. Zamiri, A. K. Zak, A. H. Abdullah and N. A. Ibrahim, Time-dependent effect in green synthesis of silver nanoparticles, *Int. J. Nanomed.*, 2011, **6**(1), 677–681, https://www.researchgate.net/publi-cation/215963324_Time-dependent_effect_in_green_synthesis_of_silver_nanoparticles.

74 M. S. H. Akash and K. Rehman, Ultraviolet-Visible (UV-VIS) Spectroscopy, in *Essentials of Pharmaceutical Analysis*, Springer Singapore, Singapore, 2019, pp. 29–56.

75 L. Mahmudin, E. Suharyadi, A. B. S. Utomo and K. Abraha, Optical Properties of Silver Nanoparticles for Surface Plasmon Resonance (SPR)-Based Biosensor Applications, *J. Mod. Phys.*, 2015, **06**(08), 1072–1074.

76 P. Roy, B. Das, A. Mohanty and S. Mohapatra, Green syn-thesis of silver nanoparticles using azadirachta indica leaf extract and its antimicrobial study, *Appl. Nanosci.*, 2017, **7**(8), 843–849.

77 J. Jalab, W. Abdelwahed, A. Kitaz and R. Al-Kayali, Green synthesis of silver nanoparticles using aqueous extract of Acacia cyanophylla and its antibacterial activity, *Heliyon*, 2021, **7**(9), 1–17.

78 M. Abd Mutalib, M. A. Rahman, M. H. D. Othman, A. F. Ismail and J. Jaafar, Scanning Electron Microscopy (SEM) and Energy-Dispersive X-Ray (EDX) Spectroscopy, in *Membrane Characterization*, Elsevier, 2017, pp. 161–179.

79 J. Schmitt and H. C. Flemming, FTIR-spectroscopy in microbial and material analysis, *Int. Biodeterior. Biodegrad.*, 1998, **41**(1), 1–11.

80 D. Karnan Singaravelu, S. Bala Subramaniyan, M. P. Tharunya and A. Veerappan, Antimicrobial lipid capped copper sulfide nanoparticles display enhanced bactericidal effect against Carbapenem-Resistant Acinetobacter baumannii, *Mater. Lett.*, 2022, **306**, 2–5.

81 H. Jia, R. Fang, J. Lin, X. Tian, Y. Zhao, L. Chen, *et al.*, Evaluation of resazurin-based assay for rapid detection of polymyxin-resistant Gram-negative bacteria, *BMC Microbiol.*, 2020, **20**(1), 13–14.

82 H. Maeda, S. Matsu-Ura, V. Yamauchi and H. Ohmori, Resazurin as an electron acceptor in glucose oxidase-catalyzed oxidation of glucose, *Chem. Pharm. Bull.*, 2001, **49**(5), 622–625.

83 P. Banerjee, M. Satapathy, A. Mukhopahayay and P. Das, Leaf extract mediated green synthesis of silver nanoparticles from widely available Indian plants: Synthesis, characterization, antimicrobial property and toxicity analysis, *Bioresour. Bioprocess.*, 2014, **1**(1), 1–10, https://bioresourcesbioprocessing.springeropen.com/articles/10.1186/s40643-014-0003-y.

84 A. Miranda, T. Akpobolokemi, E. Chung, G. Ren and B. T. Raimi-Abraham, pH Alteration in Plant-Mediated Green Synthesis and Its Resultant Impact on Antimicrobial Properties of Silver Nanoparticles (AgNPs), *Antibiotics*, 2022, **11**(11), 1592, https://pubmed.ncbi.nlm.nih.gov/36358247/.

85 T. Klar, M. Perner, S. Grosse, G. von Plessen, W. Spirkl and J. Feldmann, Surface-Plasmon Resonances in Single Metallic Nanoparticles, *Phys. Rev. Lett.*, 1998, **80**(19), 4247–4249, https://journals.aps.org/prl/abstract/10.1103/PhysRevLett.80.4249.

86 K. A. Willets and R. P. Van Duyne, Localized surface plasmon resonance spectroscopy and sensing, *Annu. Rev. Phys. Chem.*, 2007, **58**, 267–297.

87 F. Lü, Y. Gao, J. Huang, D. Sun and Q. Li, Roles of biomolecules in the biosynthesis of silver nanoparticles: Case of gardenia jasminoides extract, *Chin. J. Chem. Eng.*, 2014, **22**(6), 706–712.

88 M. Thirunavoukkarasu, U. Balaji, S. Behera, P. K. Panda and B. K. Mishra, Biosynthesis of silver nanoparticle from leaf extract of Desmodium gangeticum (L.) DC. and its biomedical potential, *Spectrochim. Acta, Part A*, 2013, **116**, 424–427.

89 A. Panáček, M. Kolář, R. Večeřová, R. Prucek, J. Soukupová, V. Kryštof, *et al.*, Antifungal activity of silver nanoparticles against Candida spp, *Biomaterials*, 2009, **30**(31), 6333–6340.

90 C.G Jones. *Scanning Electron Microscopy: Preparation and Imaging for SEM*. 2012. p. 1–20.

91 E. P. C. Mes, W. T. Kok, H. Poppe and R. Tijssen, Comparison of methods for the determination of diffusion coefficients of polymers in dilute solutions: The influence of polydispersity, *J. Polym. Sci., Part B*, 1999, 593–603, https://onlinelibrary.wiley.com/doi/abs/10.1002/(SICI)1099-0488(19990315)37:6%3C593::AID-POLB11%3E3.0.CO;2-N.

92 S. Bhattacharjee, DLS and zeta potential - What they are and what they are not?, *J. Controlled Release*, 2016, **235**, 337–351, https://pubmed.ncbi.nlm.nih.gov/27297779/.

93 D. Sharma, D. Maheshwari, G. Philip, R. Rana, S. Bhatia, M. Singh, R. Gabrani, S. K. Sharma, J. Ali, R. K. Sharma and S. Dang, Formulation and Optimization of Polymeric Nanoparticles for Intranasal Delivery of Lorazepam Using Box-Behnken Design: *In Vitro* and *In Vivo* Evaluation, *BioMed Res. Int.*, 2014, 156010.

94 J. Stetefeld, S. A. McKenna and T. R. Patel, Dynamic light scattering: a practical guide and applications in biomedical sciences, *Biophys. Rev.*, 2016, **8**, 409–427.

95 F. Lü, Y. Gao, J. Huang, D. Sun and Q. Li, Roles of Biomolecules in the Biosynthesis of Silver Nanoparticles: Case of Gardenia jasminoides Extract, *Chin. J. Chem. Eng.*, 2014, **22**(6), 706–712.

96 J. Schmitt and H. C. Flemming, FTIR-spectroscopy in microbial and material analysis, *Int. Biodeterior. Biodegrad.*, 1998, **41**(1), 1–11.

97 B. K. Mandal, R. Mandal, D. Limbu, M. D. Adhikari, P. S. Chauhan and R. Das, Green synthesis of AgCl nanoparticles using Calotropis gigantea: Characterization and their enhanced antibacterial activities, *Chem. Phys. Lett.*, 2022, 2–5.

98 E. Kohan Baghkheirati, M. B. Bagherieh-Najjar, H. Khandan Fadafan and A. Abdolzadeh, Synthesis and antibacterial activity of stable bio-conjugated nanoparticles mediated by walnut (Juglans regia) green husk extract, *J. Exp. Nanosci.*, 2016, **11**(7), 512–517.

99 N. Ramamurthy and S. Kannan, Fourier transform infrared spectroscopic analysis of a plant (Calotropis gigantea Linn) from an industrial village, Cuddalore dt, Tamilnadu, India, *Rom. J. Biophys.*, 2007, **17**, 2–8.

100 K. Ding, S. Liang, C. Xie, Q. Wan, C. Jin, S. Wang, *et al.*, Discrimination and Quantification of Soil Nanoparticles by Dual-Analyte Single Particle ICP-QMS, *Anal. Chem.*, 2022, **94**(30), 10745–10753, https://pubs.acs.org/doi/full/10.1021/acs.analchem.2c01379.

101 M. V. Balarama Krishna, D. Karunasagar and J. Arunachalam, Studies on the determination of trace elements in high-purity Sb using GFAAS and ICP-QMS, *Fresenius' J. Anal. Chem.*, 1999, **363**(4), 353–358, https://link.springer.com/article/10.1007/s002160051202.

102 R. S. Houk, V. A. Fassel, G. D. Flesch, H. J. Svec, A. L. Gray and C. E. Taylor, Inductively Coupled Argon Plasma as an Ion Source for Mass Spectrometric Determination of Trace Elements, *Anal. Chem.*, 1980, **52**, 2283–2289, https://pubs.acs.org/sharingguidelines.

103 V. Kumar, A. K. Chopra and S. Srivastava, Assessment of Heavy Metals in Spinach (Spinacia oleracea L.) Grown in Sewage Sludge–Amended Soil, *Commun. Soil Sci. Plant Anal.*, 2016, **47**(2), 221–236.

104 A. I. Ambo, O. Patience and E. B. Ayakeme, Evaluation of the proximate composition and metal content of spinach (Spinacia oleracea) from selected towns in Nasarawa State, Nigeria, *Sci. World J.*, 2023, **18**(1), 26–30, https://www.ajol.info/index.php/swj/article/view/246288.

105 S. Akter, S. M. Fahad, S. S. Ashrafi, M. J. Abedin, Y. N. Jolly, M. J. Kabir, *et al.*, Elemental Analysis of Basella alba, Spinacia oleracea, Abelmoschus esculentus (L.), Ipomoea aquatica, Colocasia esculenta, Amaranthus dubius, and Raphanus sativus Vegetables Using the PIXE

Technique in a Saline Region of Bangladesh, Rampal Area, *Biol. Trace Elem. Res.*, 2022, **200**(6), 2999–3008, https://link.springer.com/article/10.1007/s12011-021-02866-0.

106 A. Miranda, T. Akpobolokemi, E. Chung, G. Ren and B. T. Raimi-Abraham, pH Alteration in Plant-Mediated Green Synthesis and Its Resultant Impact on Antimicrobial Properties of Silver Nanoparticles (AgNPs), *Antibiotics*, 2022, **11**(11), 1592, https://pmc/articles/PMC9686503/.

107 A. K. Giri, B. Jena, B. Biswal, A. K. Pradhan, M. Arakha, S. Acharya, *et al.*, Green synthesis and characterization of silver nanoparticles using Eugenia roxburghii DC. extract and activity against biofilm-producing bacteria, *Sci. Rep.*, 2022, **12**(1), 1–9, https://www.nature.com/articles/s41598-022-12484-y.

108 W. A. Lotfy, B. M. Alkersh, S. A. Sabry and H. A. Ghozlan, Biosynthesis of Silver Nanoparticles by Aspergillus terreus: Characterization, Optimization, and Biological Activities, *Front. Bioeng. Biotechnol.*, 2021, **9**, 633468.

109 K. Ssekatawa, D. K. Byarugaba, C. D. Kato, E. M. Wampande, F. Ejobi, J. L. Nakavuma, *et al.*, Green Strategy–Based Synthesis of Silver Nanoparticles for Antibacterial Applications, *Front. Nanotechnol.*, 2021, **3**, 1–7.

110 Z. Niu and Y. Li, *Removal and utilization of capping agents in nanocatalysis*, Chemistry of Materials, 2014, vol. 26, pp. 72–83.

111 S. Kaliyaperumal and M. Radhika, Study of phytochemical analysis and antioxidant activity of Spinach oleracea L plant leaves, *Int. J. Pharmacogn.*, 2020, **7**(7), 1–4.

112 A. D. Olasupo, A. B. Aborisade and O. V. Olagoke, Phytochemical Analysis and Antibacterial Activities of Spinach Leaf, *Am. J. Phytomed. Clin. Ther.*, 2018, **6**(2), 8, https://www.imedpub.com/phytomedicine-and-clinical-therapeutics/iMedPubJournalswww.imedpub.com.

113 S. M. Fahad, A. F. M. M. Islam, M. Ahmed, N. Uddin, M. R. Alam, M. F. Alam, *et al.*, Determination of elemental composition of Malabar spinach, lettuce, spinach, hyacinth bean, and cauliflower vegetables using proton induced X-Ray emission technique at Savar subdistrict in Bangladesh, *BioMed Res. Int.*, 2015, **2015**, 1–8.

114 S. Chandra, S. Mishra and P. Darshan, Detection of heavy metals and elements via SEM technique in green leafy vegetables, *J. Chem. Inf. Model.*, 2019, **2**(1), 54–57.

115 T. C. Dakal, A. Kumar, R. S. Majumdar and V. Yadav, Mechanistic basis of antimicrobial actions of silver nanoparticles, *Front. Microbiol.*, 2016, **7**, 1–12.

116 K. Zawadzka, K. Kaİ§dzioła, A. Felczak, N. Wrońska, I. Piwoński, A. Kisielewska, *et al.*, Surface area or diameter - Which factor really determines the antibacterial activity of silver nanoparticles grown on TiO2 coatings?, *New J. Chem.*, 2014, **38**(7), 3275–3281.

117 A. O. El-Gendy, A. Samir, E. Ahmed, C. S. Enwemeka and T. Mohamed, The antimicrobial effect of 400 nm femtose-

cond laser and silver nanoparticles on Gram-positive and Gram-negative bacteria, *J. Photochem. Photobiol., B*, 2021, **223**, 112300.

118 P. R. More, S. Pandit, A. De Filippis, G. Franci, I. Mijakovic and M. Galdiero, Silver Nanoparticles: Bactericidal and Mechanistic Approach against Drug Resistant Pathogens, *Microorganisms*, 2023, **11**(2), 369, https://www.mdpi.com/2076-2607/11/2/369/htm.

119 I. X. Yin, J. Zhang, I. S. Zhao, M. L. Mei, Q. Li and C. H. Chu, The Antibacterial Mechanism of Silver Nanoparticles and Its Application in Dentistry, *Int. J. Nanomed.*, 2020, **15**, 2555–2562, https://pmc/articles/PMC7174845/.

120 Y. Y. Loo, Y. Rukayadi, M. A. R. Nor-Khaizura, C. H. Kuan, B. W. Chieng, M. Nishibuchi, *et al.*, In Vitro antimicrobial activity of green synthesized silver nanoparticles against selected Gram-negative foodborne pathogens, *Front. Microbiol.*, 2018, **9**(Jul), 1555.

121 Global tuberculosis report, 2023, 1–11, https://iris.who.int/.

122 E. McGraw, R. H. Dissanayaka, J. C. Vaughan, N. Kunte, G. Mills, G. M. Laurent, *et al.*, Laser-Assisted Delivery of Molecules in Fungal Cells, *ACS Appl. Bio Mater.*, 2020, **3**(9), 6167–6176, https://pubs.acs.org/doi/full/10.1021/acsabm.0c00720.

123 A. J. P. Brown, P. Alistair and C. J. Brown, Fungal resilience and host–pathogen interactions: Future perspectives and opportunities, *Parasite Immunol.*, 2023, **45**(2), 1–15, https://onlinelibrary.wiley.com/doi/full/10.1111/pim.12946.

124 H. T. Taff, K. F. Mitchell, J. A. Edward and D. R. Andes, Mechanisms of Candida biofilm drug resistance, *Future Microbiol.*, 2013, **8**(10), 1325–1337.

125 A. H. Hashem, E. Saied, B. H. Amin, F. O. Alotibi, A. A. Al-Askar, A. A. Arishi, *et al.* Antifungal Activity of Biosynthesized Silver Nanoparticles (AgNPs) against Aspergilli Causing Aspergillosis: Ultrastructure Study, *J. Funct. Biomater.*, 2022, **13**(4), 2, https://pmc/articles/PMC9680418/.

126 L. Zhou, X. Zhao, M. Li, Y. Lu, C. Ai, C. Jiang, *et al.*, Antifungal activity of silver nanoparticles synthesized by iturin against Candida albicans in vitro and in vivo, *Appl. Microbiol. Biotechnol.*, 2021, **105**(9), 3759–3770, https://link.springer.com/article/10.1007/s00253-021-11296-w.

127 I. Akpinar, M. Unal and T. Sar, Potential antifungal effects of silver nanoparticles (AgNPs) of different sizes against phytopathogenic Fusarium oxysporum f. sp. radicis-lycopersici (FORL) strains, *SN Appl. Sci.*, 2021, **3**(4), 1–9, https://link.springer.com/article/10.1007/s42452-021-04524-5.

128 L. Li, H. Pan, L. Deng, G. Qian, Z. Wang, W. Li, *et al.*, The antifungal activity and mechanism of silver nanoparticles against four pathogens causing kiwifruit post-harvest rot, *Front. Microbiol.*, 2022, **13**, 1–12.